

Thermal oxidation of Ge-implanted Si: Role of defects

S.N. Dedyulin*, L.V. Goncharova

Department of Physics and Astronomy, The University of Western Ontario, London, Ontario, Canada N6A 3K7

ARTICLE INFO

Article history:

Available online 17 February 2011

Keywords:

SiGe
Thermal oxidation
Defects

ABSTRACT

Thermal oxidation of Ge-implanted Si (SiGe) was carried out in dry O₂ at 1073, 1173, and 1273 K for various times. Rutherford backscattering spectrometry in random and channeling geometry was used to characterize the SiO₂ thickness and composition of the Si_{1-x}Ge_x layer to determine the oxidation kinetics and to monitor changes in the Ge distribution in the implanted layer. Oxide thicknesses obtained in this work were compared with published results for SiGe from the Deal and Grove (DG) model perspective with modified constants for SiGe oxidation. Reasonable agreement between the data and the “ideal” DG curve is achieved, namely, the residuals are randomly scattered around zero, but the results of a statistical test suggest that the DG model equation explains only 70% of the variation of the data. The possible influence of point defects in implanted samples on the oxidation rate was further tested by preannealing the implantation damage. It was found that oxide thicknesses measured for preannealed samples differ from those for as implanted samples by less than 10%, which cannot explain the observed discrepancies with the DG model. We thus suggest that the implantation damage is being annealed during the thermal oxidation itself.

© 2011 Elsevier B.V. All rights reserved.

1. Introduction

In the last decade silicon–germanium (SiGe) alloys have been implemented in the current semiconductor technology and numerous publications have been dedicated to their properties [1,2]. Yet questions regarding the SiGe oxidation mechanism still remain. SiGe oxidation has been studied under a variety of oxidation conditions: at atmospheric pressure and elevated temperature [3–18], and at high oxygen pressure [6,19], using microwave oxygen plasma [20], ultraviolet ozone [21], or rapid thermal oxidation [22,23]. The oxidation experiments were performed in pure O₂ (dry oxidation) [3,4,8,9,13–17] or by bubbling N₂/O₂ through H₂O (wet oxidation) [5–7,9–12,18]. In these studies SiGe thin films were obtained by different growth techniques such as chemical vapor deposition (CVD) [4–6,19,12], molecular beam epitaxy (MBE) [7,8,14,19,21–23], physical evaporation [3,18] as well as Ge ion implantation in Si [9–11,13,15–17]. Despite the great differences in the preparation of SiGe samples and oxidation procedures, the main features of SiGe thermal oxidation may be summarized by the following:

- Pure SiO₂ was formed during oxidation: Ge atoms that were rejected from the growing silicon oxide piled up at the interface. This was observed in all cases, unless the temperature was low enough (≤ 973 K) [24], or the oxidation pressure was high

[6,19], or the Ge concentration, x , in the alloy satisfied $x \geq 0.5$ [7,8], or the oxidation time was very short [22,23]. All these conditions prevent Ge diffusion away from the reacting interface.

- The oxidation rate of SiGe in a wet atmosphere was enhanced in comparison to pure Si [4,5,9–12,18,25], while there was no enhancement in the dry O₂ [9,16,22,25] (unless the sample was first pre-enriched with Ge to form approximately one monolayer of Ge at the interface [9]).
- Oxidation rate enhancement occurs during an initial linear regime of oxide growth [10].

SiGe oxidation rate enhancement has been explained by: (i) the weaker Si–Ge bond [11], (ii) Ge catalytic role for oxidation reaction [12], and (iii) changes in defect generation at the reacting interface [12]. It was shown for Ge ion implanted samples that the Deal and Grove model (DG model) for Si oxidation can still be applied with the linear B/A constant modified to take into account enhanced oxidation kinetics at the SiGe/SiO₂ interface [9,10,13].

The DG model for Si thermal oxidation [26] assumes that the oxidation occurs by diffusion of the oxidant to the SiO₂/Si interface where it reacts with Si. The oxidation rate is described by the parabolic equation:

$$x_0^2 + Ax_0 = B(t + \tau), \quad (1)$$

where x_0 is the oxide thickness, t is the oxidation time, A and B are constants for a given set of oxidation conditions, and $\tau = \frac{x_0^2 + Ax_0}{B}$ is the shift in the time coordinate due to the presence of the initial oxide layer, x_i . Two different growth regimes are usually considered: a

* Corresponding author.

E-mail addresses: sdedyuli@uwo.ca (S.N. Dedyulin), lgonchar@uwo.ca (L.V. Goncharova).

linear regime where $t \ll A^2/4B$ that leads to the relation $x_0 = \frac{B}{A}(t + \tau)$ and a parabolic regime where $t \gg A^2/4B$ and $x_0^2 = Bt$ for the oxide thickness. In the DG model the growth rates in the linear and parabolic regimes of growth are controlled by interface reaction and diffusion of the oxidant through the oxide layer, respectively. As proposed by Deal and Grove, the linear constant B/A is relevant to the processes at the SiO_2/Si interface via the oxidation reaction rate at the interface. The parabolic constant B refers to the properties of the oxidant in the oxide layer via a dependence on the diffusion coefficient. A new model for Si oxidation has been recently suggested [27]. Despite using the same parabolic equation as in the DG model (Eq. (1)), Watanabe et al. arrive at this result from totally different assumptions. Namely, Watanabe et al. assume that diffusivity is suppressed in the strained oxide region (≈ 1 nm) near the SiO_2/Si interface. This assumption leaves Eq. (1) and the parabolic B constant unmodified and does not treat the interface reaction as a limiting stage.

So far, no attempt has been made to consider a possible influence of the defects in the SiGe layer on the oxidation rate. Therefore, the aim of this work is to analyze published results regarding only the dry SiGe oxidation from the DG model point of view and explore the influence of point defects on the oxidation rate of Ge ion-implanted Si samples. Ion implantation is believed to produce a relatively high and well predicted initial concentration of point defects in comparison with SiGe thin film deposition techniques (e.g., MBE). Rutherford backscattering spectrometry (RBS) in random and channeling geometry is used to characterize the SiO_2 thickness and the composition of the $\text{Si}_{1-x}\text{Ge}_x$ layer to determine the oxidation kinetics and to monitor changes in the Ge distribution in the implanted layer.

We found that thermal oxidation kinetics of SiGe can be approximately described by a simple Deal and Grove model equation $x_0^2 + Ax_0 = B(t + \tau)$. The initial high concentration of point defects in the implanted SiGe layer increases the oxidation rate only slightly. Thus, annealing of the implantation damage decreases the oxide thickness by less than 10%. The latter result can be explained by taking into account initial Ge and point defect distributions in the implanted layer and including the assumption about partial annealing of the implantation damage during the oxidation process itself. We compare our results with earlier publications on the oxidation rate in the SiGe system.

2. Experiment

Czochralski (001) Si single crystals (n-doped, 1–15 Ω cm) were implanted with Ge ions at an energy of 25 keV and to a fluence of $1 \times 10^{15} \text{ cm}^{-2}$. The implantation was performed at room temperature with a sample tilted by 60° at 10^{-7} Torr.

The as-implanted samples were oxidized in dry O_2 at 1273 K for 30, 60, 120 and 180 min and at 1173 and 1073 K for 60 min along with pure reference Si samples (to ensure accurate comparison of the oxidation effects) in a quartz-tube furnace using a quartz boat. The furnace was pumped down to ≈ 25 mTorr prior to annealing to remove residual oxygen and water vapor traces, thereby preventing oxidation during the temperature ramp. To remove implantation damage, selected samples were preannealed in N_2 or in forming gas (4.96% H_2 in N_2) in a tube furnace for 30 min at 1273 K or in a Rapid Thermal Annealer (RTA) for 10 min at 1373 K in dry N_2 atmosphere.

The RBS was performed for several spots on the sample to check the uniformity of the oxide layer. Rotating random and channeling incidence along the [100] crystallographic direction with a detector mounted at 170° were done using a 1.5 MeV $^4\text{He}^+$ ion beam. A Bi-implanted amorphous silicon sample with a known total ^{209}Bi content of $4.81 \times 10^{15} \text{ atoms/cm}^2$ located ≈ 16 nm below the

surface was used to determine the detector solid angle and accurately monitor the variation of Ge content. Backscattered ion energy distributions were simulated using SIMNRA software, v. 6.05 [28] and the information on the Ge dose, Ge segregation, diffusion, crystal quality and oxide thickness were determined.

3. Results and discussion

All the RBS spectra measured for Ge-implanted samples contain the main features widely discussed in the literature (see Section 1): namely, Ge piles up at the SiGe/SiO_2 interface and pure SiO_2 is formed. The kinetic curve for SiGe samples oxidized at 1273 K in dry O_2 are presented in Fig. 1 together with data obtained for pure Si oxidized under the same conditions. We conclude that there is no enhancement in the oxidation rate within the experimental uncertainty, as one might expect from the experimental conditions used in this work. In contrast, the oxidation enhancement in dry O_2 of approximately 10–20 nm was reported in [4,14] for the samples with the low Ge content. This may be simply due to the lateral non-homogeneity of oxide thickness along the sample surface or due to other experimental discrepancies (see further discussion below). The last statement is difficult to verify since a discussion of experiments where the oxide thickness is measured by different techniques is beyond the scope of this work.

Oxide thicknesses obtained here were compared with published results for SiGe dry oxidation only. The comparison curve is presented in Fig. 2. The data are plotted using normalized coordinates [26]: $X = 4B(t + \tau)/A^2$ and $Y = 2x_0/A$ in which Eq. (1) is simply $Y^2 + 2Y = X$. This approach allows one to account for both differences in oxidation temperature and enhancement in the oxidation rate, but not for the differences in Ge concentrations between sets of samples. Modified A and B constants have been taken directly from [9] or calculated using activation energies as reported in [13,26] and using the Arrhenius equation. For comparison, the “ideal” DG curve is also shown. Note that many references lack some experimental details and/or values of measured oxide thicknesses: therefore they cannot be included in this analysis which may explain the scarcity and dispersion of the data points.

Reasonable agreement between the data points and the “ideal” DG curve is achieved, where the residuals appear to be randomly scattered around zero. The latter observation is a first indication that the model describes the data well. But the results of a R -square statistical test suggest that the DG model equation explains only

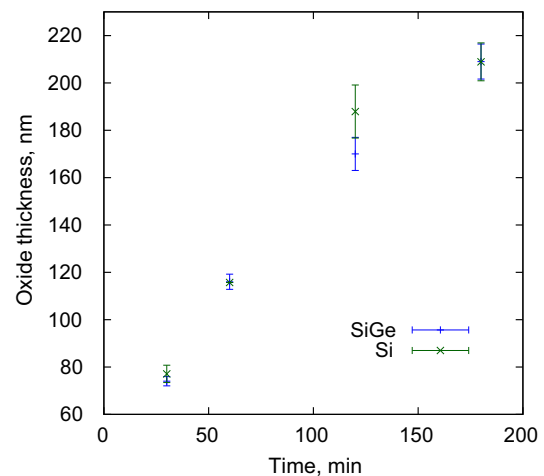


Fig. 1. Silicon oxide thickness as a function of oxidation time for Si and SiGe samples oxidized at 1273 K in dry O_2 . Thicknesses are measured from RBS spectra assuming SiO_2 stoichiometry.

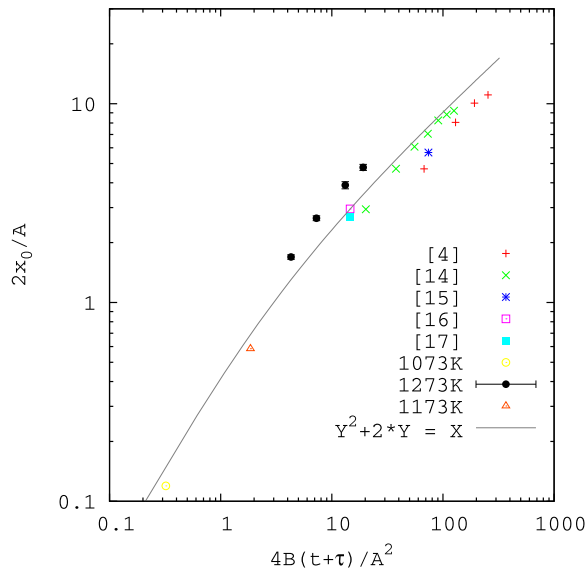


Fig. 2. Thermal oxidation of SiGe in dry O₂. The solid line represents the DG model [26]. Experimental and literature data were reduced using values of *A* and *B* determined in [9]. Modified *A* constant has been used in the case of the reported oxidation rate enhancement.

Table 1
Comparison of preannealed and as-implanted SiGe samples. Values of %Ge are given with an uncertainty of 13%.

	% of Ge _{Si}	% of Ge loss	SiO ₂ areal density (10 ¹⁵ at/cm ²)
SiGe as implanted	13	N/A	890
N ₂ anneal	87	– ^a	830
Forming gas anneal	86	0	840
RTA	49	0	830

^a Corresponding number was not calculated due to the high background between Si edge and Ge peak in RBS spectra.

70% of the variation of the data (for a list of possible reasons see below). On the another hand, for dry oxidation, low Ge concentration and high oxidation temperatures (see Section 1), pure Si and SiGe have basically the same oxidation rate and one might simply use the original *A* and *B* constants derived by Deal and Grove for pure Si [26]. But in this case the residuals, which are systematically positive for much of the data range indicate a poor fit for the data. For further proof of the validity of the first approach, longer oxidation times (e.g. 10¹–10³ h) are needed.

In summary, our results show that the DG model equation correctly predicts the tendency of changing SiGe oxide thickness with oxidation time. The observed discrepancies may be due to the following:

- Ge concentrations varied within the range 1–40 at.% range in all the samples tested in our work and reported previously. However, the *A* and *B* coefficients from [9], which are referenced to a specific Ge concentration (i.e., 80 keV Ge⁺ ion implantation to a fluence of 2 × 10¹⁶ cm⁻²), may differ for changed Ge content.
- Different experimental techniques may give unlike absolute values of oxide thicknesses. Note that simulations of RBS spectra allow one to determine the oxide thickness with an accuracy better than 2–3 nm due to the well established scattering cross sections at the energy used in this experiment and due to the presence of three reference points used for the fitting: (i) shift

of the Ge peak position due to the segregation (see Section 1), (ii) shift of the step-like feature on the Si edge due to the oxidation, and (iii) oxygen peak area. The ideal fit describes all three reference points and gives the total high accuracy of the measurement. In addition, RBS avoids assumptions related to structure-dependent parameters, i.e. the refractive index of the growing oxide as used in ellipsometry.

- Finally, there is an increase in the number of defects due to the implantation damage in Ge-implanted samples. In this case, *A* and *B* constants derived for ion implanted samples may not be applicable to samples grown by CVD and MBE techniques.

Oxide thicknesses for the samples oxidized at 1273 K in the current work are higher than those predicted by the DG model for the same oxidation times; measurement errors cannot account for this difference (uncertainties are smaller than the size of the symbols used). In order to search for an influence of the implantation damage occurring during sample preparation on the oxidation rate, we preannealed some of the samples as described in Section 2 and compared the oxide thicknesses with as-implanted samples. The Ge loss during the anneal may be of concern, but in all cases it was insignificant as indicated in Table 1.

Ion implanted samples usually contain an increased number of point defects in comparison with MBE or CVD samples. In the case of SiGe, these defects are correspondingly host atom vacancies (V_{Si}), knocked-on host atoms (Si_i), implanted atom interstitials (Ge_i), as well as Ge atoms on Si lattice sites (Ge_{Si}) or some combination of these four sources. The implanted ion and vacancy distributions were calculated using SRIM [29] and are presented in Fig. 3. Though SRIM correctly predicts the Ge implanted ion profile in Si, we expect that values for the number of vacancies and displaced Si atoms may exceed the actual values by an order of magnitude since SRIM does not model well the recombination of defects during implantation and thermal diffusion effects (all the simulations are done at 0 K) [29]. As indicated in Fig. 3, one should expect the maximum vacancy concentration to occur at ~6 nm, with a relatively large number of vacancies throughout the entire implanted region (at the surface ~80% of the maximum value). The latter fact is confirmed by the presence of a thin amorphous Si layer (~40 nm thick) with a Ge projected range of ~10 nm, as indicated by RBS.

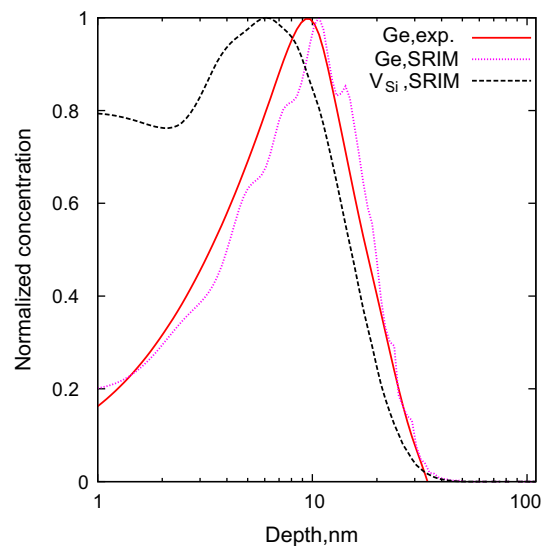


Fig. 3. Depth profile of Ge implanted in Si at 25 keV, 60° off normal. SRIM profiles for implanted Ge and Si vacancies are shown for comparison. All curves are normalized to 1 and a logarithmic scale is used for clarity.

By comparing the Ge peaks in RBS spectra obtained for random and channeling geometries, we were able to estimate the number of substitutional Ge atoms in Si. As indicated by column 1 in Table 1, a long anneal in N₂ or forming gas allows one to force Ge onto the Si crystalline positions, thereby healing the implantation damage. However, the oxide thicknesses measured for preannealed samples differ from those for as implanted sample by less than 10% (≈ 8 nm). This result cannot account for the difference with the values predicted by the DG model (Fig. 2). In this model, as discussed in Section 1, the switch between the linear and parabolic regime of growth happens for an oxidation time $t \gg A^2/4B$, which is ≈ 10 min at 1273 K. The system exists in the linear regime of oxide growth for at least 2–3 min with the linear constant $A/B = 2.17$ nm/min. We thus suggest that the implantation damage may be annealed during the thermal oxidation itself, before the region with maximum vacancy and/or Ge concentration (Fig. 3) is reached. Further investigation with an alternative oxidation mechanism (electrochemical oxidation, liquid O₂ oxidation) is needed, since simply lowering the temperature will only increase the time needed for the oxide/SiGe to move to the highly damaged region and therefore will increase the annealing time itself. Our finding does not exclude other possibilities, namely the use of the wrong A and B coefficients, taken for now from the work of [9], or the wrong assumption concerning the validity of the DG model for SiGe oxidation for short times.

4. Conclusions

Ge-implanted Si samples were oxidized in dry O₂ at 1273 K for 30–180 min and at 1073/1173 K for 60 min. Obtained oxide thicknesses were compared with published results in the framework of the DG oxidation model for pure Si with modified constants for SiGe. The R -square statistical test suggests that the DG model equation explains only 70% of the variation of the data. Therefore the hypothesis of a possible influence of the defects on the oxidation rate was tested by preannealing the samples and it was shown that oxide thicknesses measured for preannealed samples differ from those for as-implanted samples by less than 10%. This result cannot account for the differences in the oxide thicknesses obtained in this work with values predicted by the DG model.

Acknowledgements

We gratefully acknowledge Jack Hendriks of the Western Tandetron Accelerator Facility for valuable help with ion implanta-

tion and RBS measurements. Special thanks are also to Dr. William Lennard for fruitful discussion and suggested corrections. Funding was provided from NSERC/CRSNG and the University of Western Ontario.

References

- [1] M.L. Lee, E.A. Fitzgerald, M.T. Bulsara, M.T. Currie, A. Lochtefeld, *J. Appl. Phys.* 97 (2005) 011101.
- [2] J.D. Cressler (Ed.), *SiGe and Si Strained-layer Epitaxy for Silicon Heterostructure Devices*, CRC Press, 2007.
- [3] Y. Zhang, C. Li, K. Cai, Y. Chen, S. Chen, H. Lai, J. Kang, *J. Appl. Phys.* 106 (2009) 06358.
- [4] C. Li, K. Cai, Y. Zhang, H. Lai, S. Chen, *J. Electrochem. Soc.* 155 (2008) H156.
- [5] M. Tanaka, T. Ohka, T. Sadoh, M. Miyao, *Thin Solid Films* 517 (2008) 251.
- [6] D.C. Paine, C. Caragianis, A.F. Schwartzman, *J. Appl. Phys.* 70 (1991) 5076.
- [7] J. Eugene, F.K. LeGoues, V.P. Kesan, S.S. Iyer, F.M. d Heurle, *Appl. Phys. Lett.* 59 (1991) 78.
- [8] H.K. Liou, P. Mei, U. Gennser, E.S. Yang, *Appl. Phys. Lett.* 59 (1991) 1200.
- [9] K. Hossain, L.K. Savage, O.W. Holland, *Nucl. Instrum. Methods B* 241 (2005) 553.
- [10] A.R. Srivatsa, S. Sharan, O.W. Holland, J. Narayan, *J. Appl. Phys.* 65 (1989) 4028.
- [11] O.W. Holland, C.W. White, D. Fathy, *Appl. Phys. Lett.* 51 (1987) 520.
- [12] F. LeGoues, R. Rosenberg, T. Nguyen, F. Himpel, B.S. Meyerson, *J. Appl. Phys.* 65 (1989) 1724.
- [13] K. Hossain, O.W. Holland, F.U. Naab, L.J. Mitchell, P.R. Poudel, J.L. Duggan, F.D. McDaniel, *Nucl. Instrum. Methods B* 261 (2007) 620.
- [14] T. Shimura, M. Shimizu, S. Horiuchi, H. Watanabe, K. Yasutake, M. Umeno, *Appl. Phys. Lett.* 89 (2006) 111923.
- [15] R. Turan, T.G. Finstad, *Semicond. Sci. Technol.* 7 (1992) 75.
- [16] A. Terrasi, S. Scalese, M. Re, E. Rimini, F. Iacona, V. Raineri, F. La Via, S. Colonna, S. Mobilio, *J. Appl. Phys.* 91 (2002) 6754.
- [17] V. Raineri, S. Lombardo, F. Iacona, F. La Via, *Nucl. Instrum. Methods B* 116 (1996) 482.
- [18] P.E. Hellberg, S.L. Zhang, F.M. d Heurle, C.S. Petersson, *J. Appl. Phys.* 82 (1997) 5773.
- [19] E.C. Frey, N. Yu, B. Patnaik, N.R. Parikh, M.L. Swanson, W.K. Chu, *J. Appl. Phys.* 74 (1993) 4750.
- [20] M. Mukhopadhyay, S.K. Ray, C.K. Maiti, D.K. Nayak, Y. Shiraki, *Appl. Phys. Lett.* 65 (1994) 895.
- [21] A. Agarwal, J.K. Patterson, J.E. Greene, A. Rockett, *Appl. Phys. Lett.* 63 (1993) 518.
- [22] D.D. Nayak, K. Kamjoo, J.C.S. Woo, J.S. Park, K.L. Wang, *Appl. Phys. Lett.* 56 (1990) 66.
- [23] M. Spadafora, G. Privitera, A. Terrasi, S. Scalese, C. Bongiorno, A. Carnera, M. Di Marino, E. Napolitani, *Appl. Phys. Lett.* 83 (2003) 3713.
- [24] W.S. Liu, E.W. Lee, M.-A. Nickolet, V. Arbert-Engels, K.L. Wang, N.M. Abuhadba, C.R. Aita, *J. Appl. Phys.* 71 (1992) 4015.
- [25] D. Fathy, O.W. Holland, C.W. White, *Appl. Phys. Lett.* 51 (1987) 1337.
- [26] B.E. Deal, A.S. Grove, *J. Appl. Phys.* 36 (1965) 3770.
- [27] T. Watanabe, K. Tatsumura, I. Ohdomari, *Phys. Rev. Lett.* 96 (2006) 196102.
- [28] M. Mayer, *SIMNRA User's Guide*, Technical Report IPP 9/113, Max-Planck-Institut für Plasmaphysik, Garching, Germany, 1997.
- [29] J.F. Ziegler, J.P. Biersack, U. Littmark, *The Stopping and Range of Ions in Solids*, Pergamon Press, New York, 1985.